

SONO-ELASTICITY: MEDICAL ELASTICITY IMAGES DERIVED FROM ULTRASOUND
SIGNALS IN MECHANICALLY VIBRATED TARGETS

Robert M. Lerner*, Kevin J. Parker**, Jarle Holen*,
Raymond Gramiak*, and Robert C. Waag**

* Department of Radiology
**Department of Electrical Engineering
University of Rochester Medical Center
Rochester, New York 14642

INTRODUCTION

Cancers of the prostate have traditionally been detected by digital palpation which identifies increased stiffness (modulus of elasticity, hardness) of the abnormal tissue. Gray-scale ultrasound is insensitive to stiffness as an imaging parameter and often fails to reveal the extent or existence of a prostate cancer. Recent developments in technology and understanding have improved the diagnostic efficacy of transrectal ultrasound for detection of early prostate cancer, but even when coupled with digital rectal examination, a significant percentage of existing carcinomas may not be recognized. This statement is based on the lower detection rates for transrectal ultrasound and digital rectal examination in screening populations (0.1-4%) as compared to autopsy series prevalence rates of approximately 30%. Recent reports suggest that early cancers of the prostate may be characterized as hypoechoic areas in the peripheral zone of the prostate (1). Others suggest that the more advanced lesions have varied appearances ranging from hypo to hyperechoic with some even showing combinations of both (2,3). Our transrectal ultrasound experience from patients with palpable cancers (which include moderately to advanced disease), suggests a varied non-specific gray-scale appearance as well, despite the uniform impression that they are all firm on digital palpation.

Recent studies imply potential for curability of carcinoma of the prostate if it is detected before it reaches 1.0 cm^3 in volume (presuming a spherical tumor, this corresponds to a 1.3 cm diameter)(4). It is suggested that biologically active carcinomas alter the supporting prostate stroma resulting in an increased modulus of elasticity which may be detected as a region of stiffness or hardness on digital rectal examination. Since not all lesions are within the range of the examining finger, nor are all lesions palpable for a variety of reasons, a sensitive and objective method for detecting abnormal regional elasticity in prostate should lead to improved detection of carcinoma of the prostate. The purpose of this research is to incorporate tissue stiffness features into ultrasound images (sono-elasticity). The concept is that stiff tissues (cancers) will respond differently to an applied mechanical vibration than normal tissues.

This approach combines external mechanical stimulation of target

tissues with Doppler ultrasound signal detection and processing to improve lesion detection, provided the lesion creates an altered region of elasticity. Stimulation of target tissues by a controlled mechanical vibration causes regions of different elasticity to respond with different displacements and velocities. The idea of characterizing tissue from the motion or mechanical response is not new but has had only limited evaluation (5-11). Ultrasound detection schemes have utilized correlations between A-lines to detect motion of cardiovascular origin, and visual analysis of M-mode waveforms have been performed to detect motion for a 1.5 Hz external vibration source. None of these techniques has reached clinical maturity because of a number of difficulties. The A-line or M-mode techniques rely primarily on echoes from speckle regions, with few discrete specular reflections available to demonstrate motion unequivocally. The changes in speckle pattern resulting from motion of the sample volumes are complex and can be difficult to interpret. The correlations may suffer from patient motion caused by respiration and other body movements. The use of cardiovascular pulses to generate internal motion is problematic because the "source function", the radial expansion of arteries, is generally of uncertain strength, and has unknown coupling to the surrounding tissues. The pulsatile movements near the arteries can be submillimeter in extent, which is well below the resolution of conventional A-line or M-mode techniques.

In comparison, our approach employs variable frequency, external, periodic pulsations and incorporates range-gated Doppler ultrasound to detect the periodic movements of tissue. The advantages can be summarized as follows:

i) External periodic pulsation applied to a specimen provides a known stimulus which can be easily recognized as distinct from other velocity (noise) sources. Sensitive coherent signal detection schemes may then be applied to improve signal to noise ratios if indicated.

ii) The Doppler detection technique is capable of resolving much smaller displacements than A-line or M-mode techniques. This results from the fact that Doppler ultrasound measures velocity (displacement times frequency for sinusoidal motion) compared with techniques which measure displacement only. At "high" frequency (1 KHz) mechanical vibration, a conventional 2 MHz Doppler ultrasound time-frequency display is capable of resolving excursions (sinusoidal displacements) on the order of 0.06 mm (12). Thus, very small vibrations in deep tissues can be measured.

iii) The Doppler detection technique is sensitive in regions of low speckle, as well as regions with specular reflectors. For example, color-coded Doppler blood flow images are derived from regions where conventional B-scan images show extremely low reflectivity. Doppler can also display multidirectional information simultaneously, which may be of value in identifying regions of relative motion.

iv) Doppler ultrasound combined with mechanical stimulation is relatively insensitive to respiratory and other gross tissue movements. This results from the examiner's ability to identify the sinusoidal Doppler ultrasound output at a given known frequency of external vibration so that motions which are not periodic at the drive frequency can be ignored.

v) A variable frequency approach maximizes the likelihood of detecting differences between normal tissue and tumor with concomitant altered elasticity, because of the possibilities of exciting "mechanical resonances". The mechanical properties of tissue include a high degree of damping, and thus, strong resonance behavior (high Q) should not be encountered. Nonetheless, the ability to change stimulation frequency may add additional information concerning the frequency dependent response of a

region, and this information can be compared with theoretical and experimental results to estimate the mechanical properties of the region.

As a result of these advantages, the combined external vibration/Doppler ultrasound detection approach appears to be a leading candidate for determining the elastic properties of discrete regions of tissue, which may permit early detection of prostate tumors and other focal abnormalities in soft tissue.

Doppler Detection of Vibration - Principles

In periodic, sinusoidal motion, an object's velocity, V , is proportional to displacement, e , times mechanical vibrational frequency, W , because velocity is the time derivative of displacement. Thus $V = e(W)$, and as mechanical vibration frequency increases, it is evident that equal velocities are generated from smaller displacements. This is the main reason why exceptionally small displacements (0.06mm) can be detected at 1 KHz (W) by conventional 2 MHz pulsed Doppler equipment.

The representation of velocities on the conventional time-frequency Doppler display is readily apparent only when low frequency mechanical vibration is employed. Specifically, when the period of mechanical vibration is longer than the FFT period of the Doppler spectrum analyzer time window, a positive and negative periodic sine wave is directly observed on the display, with the peak frequency shifts proportional to the peak velocity according to the Doppler formula. However, at high vibrational frequencies, when the period of mechanical oscillation is much shorter than the FFT window, analysis shows that a Fourier Series solution to the Doppler shifted signal is obtained, and the time-frequency display therefore shows continuous (in the time domain) equally spaced (in the frequency domain) bands of both positive and negative Doppler-shifted frequencies. In this regime, the peak vibrational velocity is indicated by the frequency shift of the highest band and peak displacement by the number of bands (12). The following quantitative considerations are germane to preliminary experiments which follow:

i) The minimum detectable velocity (of vibrations) is influenced by the high pass filter required on all Doppler outputs to eliminate strong DC signal and low frequency "noise". We have found 333 Hz to be a reasonable cut-off in experiments, and given the Doppler carrier frequency (2-5 MHz typical) the minimum velocity is proportional to the inverse of the vibration frequency. Some typical examples are: min velocity 12.5 cm/sec (2 MHz carrier) corresponding to 1 mm displacements at low frequency, 18 Hz vibration; or 5 cm/sec (5 MHz carrier) corresponding to 0.01 mm displacements at higher frequency 1 KHz vibration.

ii) The maximum detectable velocity in pulsed Doppler systems is limited by the well known requirement that the pulse repetition frequency (PRF) be twice the expected maximum Doppler frequency (13,14). The PRF is limited by the need for unambiguous depth resolution so a velocity depth product maximum can be established. For example, with a maximum depth of 8 cm expected, the maximum resolvable velocities are on the order of 70 cm/sec for 5 MHz carrier, to 175 cm/sec for 2 MHz carrier.

Preliminary Experiments - Doppler Detection of Vibration

A specially constructed, motorized, offset-cam plunger (1 cm diameter) was used to vibrate phantoms at 18 Hz, with a plunger excursion of ± 2.5 mm. A submerged, degassed, sealed, moderately stiff sponge was utilized in one set of experiments. The sponge had a 2 cm embedded region of RTV silicone (a relatively harder "tumor" region) which had been injected in a central position before hardening occurred. Fig. 1 shows a 2.5 MHz B-scan

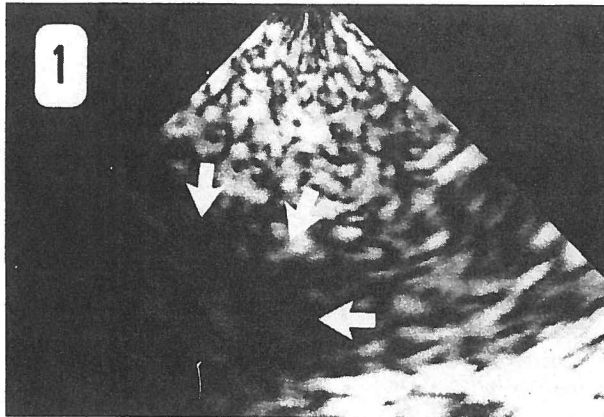


Figure 1. 2.5 MHz B-scan image of sponge phantom with stiff, RTV "tumor" embedded (arrow-heads). The higher attenuation within the RTV results in some shadowing (lower left). The overall configuration corresponds to that of Figure 2.

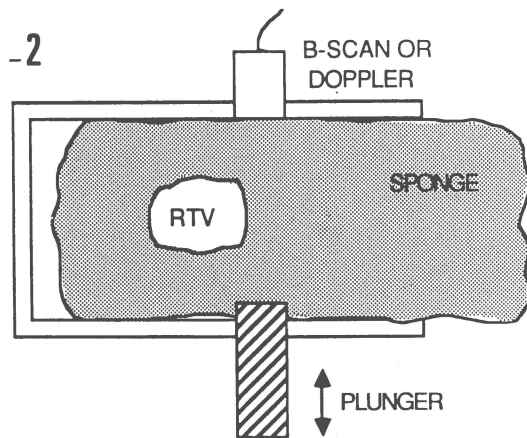


Figure 2. Schematic illustration of inhomogeneous sample with mechanical vibration and B-scan imaging or Doppler range gate measurement.

(Toshiba*) of the sponge RTV region. Shadowing occurs from the high attenuation within the RTV. However we verified that the 2 MHz Doppler transducer (Vingmed**) was able to detect motion within and distal to the hypoechoic RTV region. The experimental configuration is shown in Fig. 2. The axis of the Doppler probe-plunger was translated across the sponge in 1 cm steps and pulse Doppler data were recorded in 0.5 cm depth increments. Typical output from the Doppler unit is shown in Fig. 3. The peak velocities were recorded as a function of range-gate position within the sponge-RTV phantom. A gray scale rendition of these data is shown in Fig. 4 with peak velocities within the sample varying linearly from white (2.5 KHz Doppler shift) to black (< 300 Hz Doppler shift).

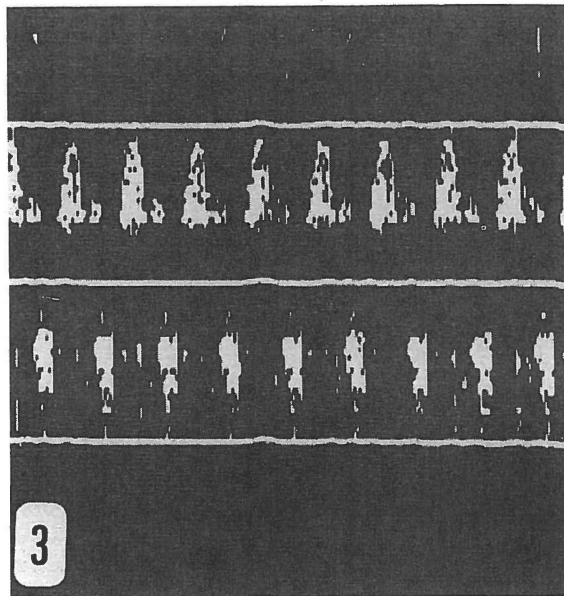


Figure 3. Output of range-gated Doppler display, with sample volume in sponge phantom subjected to 18 Hz vibration. Horizontal axis-time, 0.5 sec shown; vertical axis - Doppler frequency shift with 1 KHz per division. For slow (less than 20 Hz) sinusoidal mechanical vibrations, the positive and negative (towards and away from the Doppler probe) pulsations are clearly seen.

*Toshiba; Tustin, California

**Vingmed; Olso, Norway

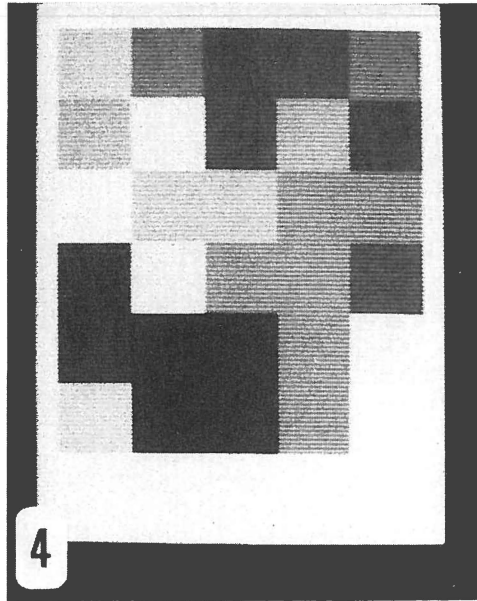


Figure 4. Computer generated image of sponge RTV phantom using range-gated Doppler peak velocities measured as a function of position. The geometry corresponds to Figures 1 and 2. Resolution is 7 blocks vertical (5mm each) by 5 blocks horizontal (roughly 1cm transverse each), thus the aspect ratio is different from Figures 1 and 2. Gray scale brightness corresponds to measured peak velocities within the sample volume, varying linearly from white (2.5 KHz Doppler shift) to black (less than 300 Hz Doppler shift). The bottom row is white due to the measurement of plunger vibration. The "tumor" region appears dark because of low peak velocities not because of its lower backscatter. This is explained by the preferential movement of the surrounding, more compliant sponge.

The bottom row is white corresponding to plunger vibration. The orientation of the computer image corresponds to Figs. 1 & 2, so the RTV "tumor" region is in the lower left hand corner. The dark region here corresponds to decreased vibration of the RTV region (due to its higher stiffness; with preferential compression of surrounding sponge), and not due to its lower backscatter coefficient, as in traditional B-scan images. Furthermore, the Doppler vibration image (sono-elasticity) (Fig 4) is quantitative, with the bottom bright regions (in this configuration) attributable directly to the plunger movement, with the gray scale in other regions representing local velocities or displacements within the phantom.

Another series of experiments examined configurations of "hard" or

"stiff" gelatin (20% gelatin, 3% formalin) vs "soft" gelatin (10% gelatin, 2% formalin), with 0.5% suspended barium sulphate particles in both for backscatter. Composite blocks were made, with 1.5 cm thickness stiff layers. Figure 5 shows the configuration (from bottom to top) of plunger; stiff layer; soft layer; and B-scan origin; where the composite image shows a 3.5 MHz B-scan image and M-mode from a centered scan line. As can be seen, the M-mode representation is difficult to quantify in speckle regions, and requires vibrations of 1 mm or greater. Fig. 6 shows the opposite configuration: plunger; soft layer; hard (stiff) layer; B-scan transducer.

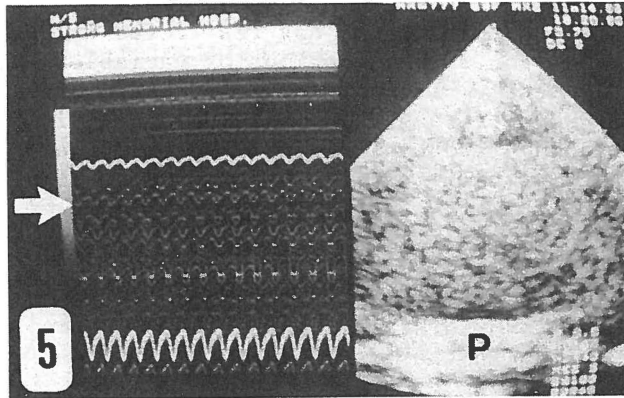


Figure 5. M-mode and B-scan images of a layered phantom. The image shown from bottom to top, the vibratory plunger (bright echo P), 2.5 cm of stiff gel and 1.5 cm of "soft" gel. The M-mode shows that the vibratory response at 2 cm distance (arrow) is of greater amplitude than in Figure 6 (below) where the vibratory stimulus first passes through a more "attenuating" 1.5 cm soft layer above the plunger.

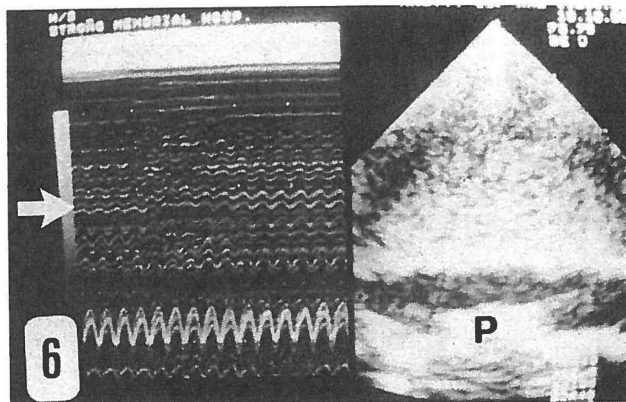


Figure 6. M-mode and B-scan images of layered phantom in reverse configuration of gel layers as compared to Figure 5. Plunger position (P) and 2 cm transmission distance (arrow) are indicated. Note that inadvertent movement of the M-mode transducer results in M-mode breakup and emphasizes difficulty, in resolving small vibrations within speckle regions by this method.

Comparing the two configurations, we see that the vibrations travel further, and with less diminuation in the hard (stiff) material than in soft, as expected from spring-mass model considerations. Fig. 6 also shows the deleterious effects of transducer movement on the M-mode - there is a pattern break-up in the center region caused by inadvertant movement of the ultrasound transducer.

In comparison, Fig. 7 shows range gated Doppler measurements of vibration within the samples, with 0.5 cm axial resolution and gray scale mapping, (corresponding to the configurations of Figs. 5 & 6). The Doppler "images" also show basic features such as the relatively uniform vibration within "hard", "stiff" layer, but rapid fall-off in the soft layer. However, the Doppler measurements are not restricted to large (1mm) displacements, and are not confused by regions of variable speckle as in the case of M-mode measurements. These preliminary results utilized prototype equipment ("Alfred"* Doppler range gate system) which did not ensure rigid Doppler probe positioning (probe vibrations are a source of noise), and used the Doppler display to visually estimate peak sinusoidal velocities.

Fig. 8 shows a halftone image of 2-D Doppler color flow image from a commercially available imager (Toshiba SSH65A). The same gelatin phantom as in Fig. 7 was scanned during low frequency vibration. The image demonstrates the feasibility of vibration imaging in real time. Different character of color coding in the two different layers was evident.

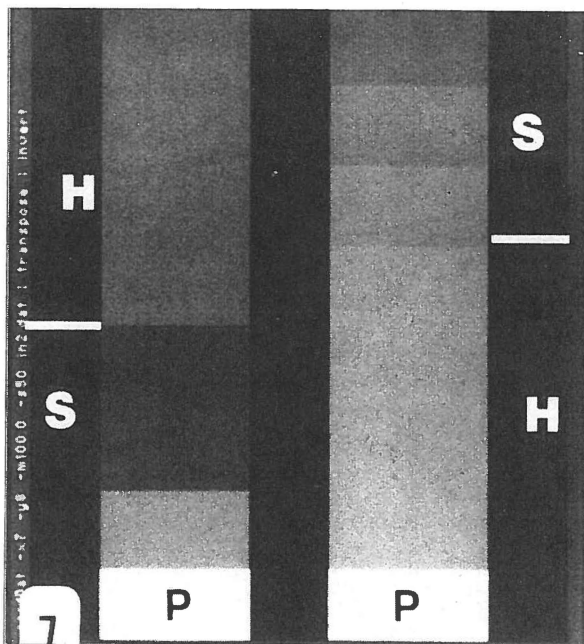


Figure 7. Gray scale image of velocity measured within vibrated, layered phantom . Doppler shift data from single scan lines through the phantom are shown (white = 2.5 KHz Doppler shift, black = below 300 Hz). Left configuration is (bottom to top) plunger (P bright sample), three range samples within "soft" gelatin layer (S), four range samples within "hard" layer (H). Each range sample corresponds to 0.5 cm distance. Right configuration is same phantom inverted.

*Alfred; Horten, Norway

In both configurations, the hard layers transmit vibrations with little loss, whereas the soft layers show rapid decay of vibrational amplitude with distance from the plunger.

The first range band in the soft layer on the left probably contains plunger movement which gives it the bright representation. The more distal samples in the soft layer show low velocity representations. More distally, in the hard layer (H) moderate velocities are represented. It would appear that the low velocities in the soft layer could result from Doppler insensitivity to off axis velocities, since a considerable amount of the plunger energy must result in movements of the soft layer particles laterally. We speculate that the recoil of the soft layer then imparts energy to the hard layer via mode conversion. The sum total of this activity is that the hard layer is stimulated to velocities which are higher than those in the soft layer in the direction of Doppler sensitivity. This concept suggests that the movement of particles in a soft layer is probably multi-directional under these stimulus conditions and that detection of motion may be possible from multiple angles.

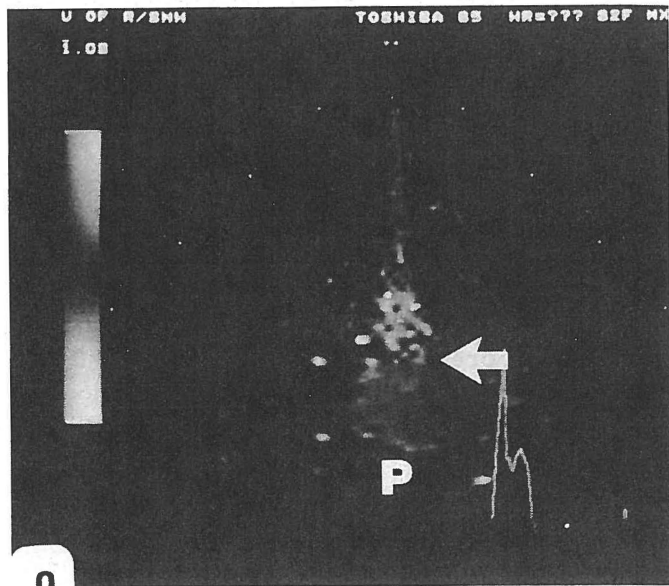


Figure 8. Halftone image representation of a color coded Doppler image of vibrated layered phantom obtained by a commercially available color flow map imager (Toshiba SSH65A). This imager is designed for cardiovascular imaging and features real time display of blood flow

Figure 8. (Continued)
motion. The sector format is evident and the relationship of the plunger (P), soft layer, and hard layer is identical to that shown in Figure 6 above. The arrow denotes the boundary between the soft layer and the hard layer. The color in the soft layer was a rather saturated red indicating that the data was obtained during movement of the plunger towards the transducer located at the apex of the scan. The homogeneity of color in the soft layer indicates that the multiple samples obtained in each beam position showed little variance in the detected flow velocity. In the hard sample, on the other hand, considerable yellow was intermixed with the red indicating that the variance was greater, a presentation which is also seen when flow velocity is increased. Although this instrument is not optimized for these investigations, it does demonstrate, real time, features of vibration in tissues.

CONCLUSION

Preliminary work using an 18 Hz mechanical vibratory system and pulsed Doppler detection has resulted in generation of prototype images of reflector or stiffness obtained from a sponge model containing a "tumor" nodule of altered stiffness. Diminished vibratory motion in the nodule is clearly evident. In another investigation, gelatin blocks of different stiffness demonstrated recognizable differences in motion of contained reflectors as well as differences in propagation of the low frequency mechanical energy transmission. These preliminary results indicate that tissue stiffness can be incorporated into gray scale ultrasound imaging.

These concepts are being applied to investigation of the prostate which should result in improved detection of carcinoma since:

1) Areas of increased stiffness/hardness not favorably located for digital rectal examination may be explored.

2) Detection of regions of altered elasticity resulting from carcinoma of the prostate should complement conventional transrectal ultrasound imaging. The ultimate goal will be to provide objective quantifiable measures of regional tissue elasticity analogous to the time honored data widely accepted in clinical circles from digital rectal palpation but produced and documented in a subjective format. Correlation of the data presented from elasticity images to data presented from conventional transrectal ultrasound and digital palpation should improve the diagnostic accuracy and confidence for specific lesions. Extension of these concepts to other organ systems follows naturally. For instance, estimates of liver fibrosis may be possible with this methodology as well as improved identification of metastatic nodules. The method may also lend itself to pressure determination in cardiac chambers and blood vessels.

REFERENCES

1. Lee F, Gray JM, McLeary RD, Meadows TR, Kumasaka GH, Borlaza GS, Straub WH, Lee, Jr., F, Solomon MH, McHugh TA, and Wolf RM: "Transrectal ultrasound in the diagnosis of prostate cancer: Location, echogenicity, histopathology, and staging", The Prostate 7:117-129, 1985.
2. Rifkin MD, Kurtz AB, Choi HY and Goldberg BB: "Endoscopic ultrasonic

- evaluation of the prostate using a transrectal probe: Prospective evaluation and acoustic characterization", Radiology, 149:265-271, 1983.
3. Burks DD, Fleischer AC, Liddell H and Kulkarni MV: "Transrectal prostate sonography: Evaluation of sonographic features in benign and malignant disease", Radiology 149:265-271, 1983.
 4. McNeal JE, Kindrachur RA, Freiha FS, Bostwick DG, Redwine EA, and Stamey TA: "Patterns of progression in prostate cancer", The Lancet pp 60-63, 1986.
 5. Rockoff SD, Green, RC, Lawson, TL, Pett, Jr., SD, Devine, III, D, and Francisco, SG: "Noninvasive measurement of cardiac pressures by induced ventricular wall resonance: Preliminary results in the dog", Investigative Radiology Vol. 13:499-505, 1978.
 6. Gore JC, Leeman S, Metreweli C, and Plessner NJ: "Dynamic autocorrelation analysis of A-scans in vivo", Ultrasonic Tissue Char. II, M. Linzer, ed. NBS special publ. 525:275-280, 1979.
 7. Wilson LS and Robinson DE: "Ultrasonic measurement of small displacements and deformations of tissue", Ultrasonic Imaging 4:71-82, 1982.
 8. Dickenson RJ and Hill CR: "Measurement of soft tissue motion using correlation between A-scans", Ultras Med. Biol 8:263-271, 1982.
 9. Eisensher A, Schweg-Toffler E, Pelletier G, and Jacquemard G: "La palpation echographique rythmee-Echosismographic", Journal de Radiologie 64:225-261, 1983.
 10. Tristram M, Barbosa DC, Cosgrove DO, Nassiri DK, Bamber JC and Hill CR: "Ultrasonic study of in vivo kinetic characteristics of human tissue", Ultrasound in Med. & Biol. Vol. 12:927-937, 1986.
 11. Yamakoshi Y, Suzuki M and Sato T: "Imaging the elastic properties using low frequency vibration and probing ultrasonic wave", Japanese Meeting of Applied Physics, Spring 1987 Tokyo.
 12. Holen J, Waag RC and Gramiak R: "Representations of rapidly oscillating structures on the Doppler display", Ultrasound in Med & Biol 11:267-272, 1985.
 13. Baker DW: "Pulsed Ultrasonic Doppler Blood Flow Sensing", IEEE Trans Sonics Ultras. SU-17(3) p 170-185, 1970.
 14. Fish PJ: "Doppler Methods", in Physical Principles of Medical Ultrasonics, C.R. Hill, Ed, Elish Horwood Ltd, Chichester, UK, 1986.